




Temperature control of nematicon trajectoriesGaetano Assanto ¹, Cassandra Khan ², Armando Piccardi,¹ and Noel F. Smyth ²¹*Nonlinear Optics and OptoElectronics Lab University of Rome "Roma Tre," Via della Vasca Navale 84, 00146 Rome, Italy*²*School of Mathematics, University of Edinburgh, Edinburgh EH9 3FD, Scotland, United Kingdom*

(Received 15 August 2019; published 13 December 2019)

Using modulation theory, we develop a simple $[(2 + 1)$ -dimensional] model to describe the synergy between the thermo-optical and reorientational responses of nematic liquid crystals to light beams to describe the routing of spatial optical solitary waves (nematicons) in such a uniaxial environment. Introducing several approximations based on the nonlocal physics of the material, we are able to predict the trajectories of nematicons and their angular steering with temperature, accounting for the energy exchange between the input beam and the medium through one-photon absorption. The theoretical results are then compared to experimental data from previous studies, showing excellent agreement.

DOI: [10.1103/PhysRevE.100.062702](https://doi.org/10.1103/PhysRevE.100.062702)**I. INTRODUCTION**

Nematicons are optical solitary waves propagating in liquid crystals in the nematic phase, i.e., with the constituent anisotropic molecules sharing the same angular orientation θ in space, but without any positional order [1]. Owing to the response of these dielectric materials to electromagnetic perturbations, linearly polarized light beams can induce self-focusing, and thereby, the generation of self-guided solitary waves in space, namely nematicons [2–6]. Such two-dimensional, $(2 + 1)$ -dimensional, all-optical self-trapped beams are essentially nondiffracting, polarization-dependent, and nonlocal with respect to the excitation wave packet and nonresonant with respect to the wavelength. For these reasons they are deemed to be ideal for the study and development of alternative generations of solitary wave-based and light controlled systems for optical signal manipulation and switching [5,7]. Numerous basic and applied features, phenomena, and potential applications of nematicons have been proposed and demonstrated [5,6]. The development of models able to describe and predict nematicon behavior and effects in various situations are therefore of importance, both theoretically and experimentally [8–24]. Notably, all such models are simplified to some extent, as the nematicon physics gives rise to nonintegrable equations which do not possess any known exact, general solitary wave solutions [7,24,25]. Despite the substantial literature on nematicons and their related theory, models describing synergetic nonlinear effects and their interplay with nematicons are scarce, as they tend to be more involved than the standard equations for nondissipative solitary waves, and thereby, less prone to general and simple solutions. Notable exceptions to this trend are recent studies of complex nematicon dynamics [26], dissipative nematicons [27], spatiotemporal nematicons [28], and light-bullet nematicon trains [29], self-focusing or defocusing effects on beam localization in nematic liquid crystals [30], and transverse fluctuations of nematicons due to correlated noise [31,32]. In this paper, we model the routing of

nematicons due to thermo-optic changes in the material properties, i.e., variations of the optical parameters of the dielectric due to the ambient temperature, as well as the (localized) heating caused by light absorption as the beam travels through the bulk medium. As recently demonstrated, such thermo-optical effects can alter the degree of nematicon confinement, its oscillatory behavior in propagation, and its trajectory [33–35]. Hereby, we adopt modulation theory [36] and develop a simple mathematical model describing temperature control of nematicon trajectories in undoped nematic liquid crystals, which includes the role of external temperature, input beam power, and one-photon absorption. This model has an exact solution. When actual material and experimental parameters are used in its solution, it is found to give excellent agreement with measured results for the dependence of beam walkoff on temperature and beam power. This specific application confirms how powerful modulation theory is in predicting the evolution of spatial solitary waves in nematic liquid crystals [7,9,11–24], even when multiple nonlinearities are present.

II. NEMATICON TRAJECTORY EQUATIONS

Let us consider the propagation of a linearly polarized, coherent light beam of wave number k_0 through a planar cell filled with nematic liquid crystals (NLC). Let us assume that the electric field E of the light beam oscillates in the x direction and that the wave packet propagates down the cell in the z direction. The y direction then completes the coordinate triad [3,7]. The cell interfaces are treated so that the molecular director lies at an angle θ_0 to the z direction in the plane (x, z) . We shall denote the extra director rotation due to the electromagnetic field by ϕ , so that the total angle of the director to z is $\theta = \theta_0 + \phi$. This configuration is sketched in Fig. 1. The refractive index eigenvalues for electric fields polarized parallel and perpendicular to the molecular director (optic axis) in the equivalent uniaxial are n_{\parallel} and n_{\perp} , respectively, with an optical anisotropy $\epsilon_a = n_{\parallel}^2 - n_{\perp}^2 > 0$. The dimensional equations governing the propagation of the beam

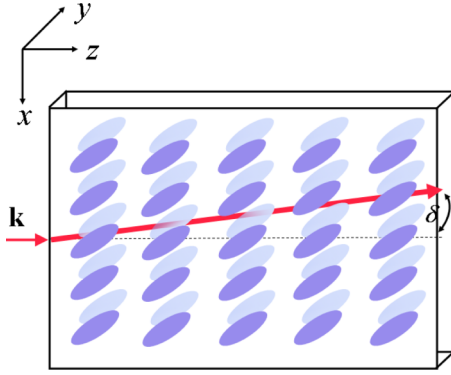


FIG. 1. Sketch of a thick planar cell showing input wave vector \mathbf{k} of the beam, extraordinary-wave walkoff $\delta = \tan^{-1} \Delta$ and preset orientation of NLC molecules.

in the NLC sample are [6]

$$2ik_0n_e \frac{\partial E}{\partial z} + 2ik_0n_e \Delta \frac{\partial E}{\partial x} + \nabla^2 E + k_0^2 [n_{\perp}^2 \cos^2 \theta + n_{\parallel}^2 \sin^2 \theta - n_{\perp}^2 \cos^2 \theta_0 - n_{\parallel}^2 \sin^2 \theta_0] E = 0 \quad (1)$$

for the electric field of the beam and

$$K \nabla^2 \theta + \frac{1}{4} \epsilon_0 \epsilon_a |E|^2 \sin 2\theta = 0 \quad (2)$$

for the reorientational response. Here K is the elastic response of the nematic liquid crystals in the single constant approximation, for which the elastic coefficients describing bend, twist, and splay deformations are assumed equal [1]. The refractive index n_e of the NLC for x -polarized electric fields at optical frequencies is given by

$$n_e^2 = \frac{n_{\perp}^2 n_{\parallel}^2}{n_{\parallel}^2 \cos^2 \theta + n_{\perp}^2 \sin^2 \theta}. \quad (3)$$

The extraordinary wave undergoes walkoff of the Poynting vector, so that the beam propagates in (x, z) at an angle $\delta = \tan^{-1} \Delta$ to the beam wave vector (i.e., the z direction), where the walkoff Δ is given by

$$\Delta = \frac{\epsilon_a \sin 2\theta}{\epsilon_a + 2n_{\perp}^2 + \epsilon_a \cos 2\theta}. \quad (4)$$

The present work is concerned with the effect of temperature on the propagation of nematicons through the sample. The light beam directly heats the medium, while the whole material is held at a fixed temperature. As the refractive indices n_{\parallel} and n_{\perp} are temperature dependent [35], the walkoff Δ and the optical anisotropy ϵ_a are also temperature dependent. Let the NLC temperature be T . The heat flow in the NLC is then governed by the (steady) forced heat equation

$$S \nabla^2 T = -\alpha \Gamma |E|^2, \quad \Gamma = \frac{1}{2} \epsilon_0 c n_e. \quad (5)$$

Here S is the thermal conductivity and α is the thermal absorption coefficient of the material.

The nematic equations (1) and (2) and the thermal equation (5) are set into nondimensional form to simplify the analysis of the nematicon trajectory. The propagation variable z is scaled by a typical length L_z , the transverse variables (x, y) are scaled by a typical width W , and the electric field is scaled by

a typical strength A_e to transform the dimensional coordinates (x, y, z) to the nondimensional coordinates (X, Y, Z) and the electric field E to the nondimensional u , with

$$z = L_z Z, \quad x = WX, \quad y = WY, \quad E = A_e u. \quad (6)$$

Suitable length scales are

$$L_z = \frac{4n_e}{(\epsilon_a)_t k_0 \sin 2\theta_0}, \quad W = \frac{2}{k_0 \sqrt{(\epsilon_a)_t} \sin 2\theta_0}. \quad (7)$$

These scalings (7) are evaluated at a typical temperature T_0 , denoted by the subscript t , as the NLC parameters are temperature dependent. The input wave packet is a Gaussian beam of power P_b , width W_b and amplitude A_e . Hence, a suitable scale for the electric field of the beam is A_e , given by

$$A_e^2 = \frac{2P_b}{\pi \Gamma W_b^2}. \quad (8)$$

Typical beams used to generate nematicons have milliwatt powers [6], with an optical reorientation ϕ much smaller than the preset θ_0 , $|\phi| \ll \theta_0$. The trigonometric functions in the nematic equations (1) and (2) are then expanded in Taylor series to $O(\phi)$. Using the scalings (7) and (8) the system (1) and (2) becomes

$$i \frac{\partial u}{\partial Z} + i\gamma \Delta(\theta_0, T) \frac{\partial u}{\partial X} + \frac{1}{2} \nabla^2 u + 2 \frac{\epsilon_a}{(\epsilon_a)_t} \phi u = 0, \quad (9)$$

$$\nu \nabla^2 \phi + 2 \frac{\epsilon_a}{(\epsilon_a)_t} |u|^2 = 0. \quad (10)$$

The nondimensional walkoff factor γ is given by

$$\gamma = \frac{2n_e}{\sqrt{(\epsilon_a)_t} \sin 2\theta_0} \quad (11)$$

and the nondimensional NLC elasticity is

$$\nu = \frac{8K}{\epsilon_0 (\epsilon_a)_t A_e^2 W^2 \sin 2\theta_0}. \quad (12)$$

The elasticity parameter ν is large, $O(100)$, for typical experimental regimes [12,37]. This regime is termed highly nonlocal and the large value of ν plays a vital role in the calculation of the nematicon trajectories below. It should be noted that the walkoff Δ has been truncated at the leading order with $\theta = \theta_0$, so that the beam self-bending due to nonlinear changes in walkoff [38,39] are ignored. This approximation has been found to give good agreement with experiments and numerical solutions for low power beams [7,40–42]. The inclusion of self-bending presents extra challenges and is the subject of current investigations.

In a similar manner the thermal equation (5) can be set in nondimensional form. Let us set A_T to be a typical temperature change from the initial temperature T_0 due to the optical heating, so that $T = T_0 + A_T \tau$, with τ the nondimensional temperature change from the background temperature T_0 . Then using the coordinate scalings (6), the thermal equation (5) becomes

$$\mu \nabla^2 \tau = -|u|^2, \quad (13)$$

where the nondimensional thermal conductivity is

$$\mu = \frac{SA_T}{\alpha\Gamma W^2 A_e^2}. \quad (14)$$

Note that the Laplacian in (13) is in the transverse variables (X, Y) . The longitudinal length of the cell is much greater than the transverse lengths, so heat preferentially flows in the transverse direction. In addition, in nondimensional variables the coefficient of τ_{ZZ} is $O(W^2/L_z^2) \ll 1$ relative to the coefficients of τ_{XX} and τ_{YY} . Equation (13) will be solved for τ for a Gaussian input beam

$$u = ae^{-r^2/w^2}, \quad (15)$$

where $r^2 = X^2 + Y^2$ is the radial distance centered on the nematicon axis. Hence the temperature change due to the light beam is described by

$$\frac{\mu}{r} \frac{\partial}{\partial r} \left(r \frac{\partial \tau}{\partial r} \right) = -a^2 e^{-2r^2/w^2}, \quad (16)$$

which has the solution

$$\tau = \frac{a^2 w^2}{4\mu} \int_{\sqrt{2} \frac{r}{w}}^{\sqrt{2} \frac{R}{w}} \frac{1 - e^{-\eta^2}}{\eta} d\eta \quad (17)$$

on assuming the fixed boundary condition $T = T_0$, $\tau = 0$, at $r = R$. Experimental cells have a rectangular cross section, but we assume the cell width much larger than the beam width, so that assuming circular symmetry is a good approximation, as will be found below. The solution (17) can now be used to determine the temperature dependence of the parameters in the nematic equations (9) and (10). This solution gives this temperature in terms of the beam power and medium parameters.

It is noted that the full system consisting of the nematic equations and the temperature equation (13) does not possess a Lagrangian representation. However, if the temperature is given as a function of (X, Y, Z) by the solution (17), then the (X, Y, Z) dependence of the refractive indices n_{\parallel} and n_{\perp} due to optical heating are established and the temperature equation (13) is not needed in the determination of the Lagrangian. The nematic equations (9) and (10) then have the Lagrangian

$$L = i(u^* u_Z - uu_Z^*) + i\gamma \Delta(\theta_0, \tau)(u^* u_X - uu_X^*) - |\nabla u|^2 + 4 \frac{\epsilon_a}{(\epsilon_a)_t} \phi |u|^2 - \nu |\nabla \phi|^2, \quad (18)$$

where the * superscript denotes the complex conjugate. To calculate the trajectory of the nematicon, this Lagrangian is “averaged” [36] by integrating in X and Y from $-\infty$ to ∞ on substituting suitable solutions u for the nematicon and ϕ for the molecular director response. This averaging treats the (slowly varying) nematicon as an equivalent mechanical particle moving in a potential and is the basis of standard solitary wave perturbation theory [24,43,44]. Unfortunately, there are no known exact nematicon solutions, besides isolated ones for fixed parameter values [25], on which to base this averaging. For this reason, let us assume the general profiles

$$u = af_e(\rho_e) e^{i\sigma + iV(X-\xi)}, \quad (19)$$

$$\phi = a_d f_d(\rho_d), \quad (20)$$

where

$$\rho_e = \frac{\sqrt{(X-\xi)^2 + Y^2}}{w}, \quad \rho_d = \frac{\sqrt{(X-\xi)^2 + Y^2}}{w_d}. \quad (21)$$

The calculation of the averaged Lagrangian can now be based on these general profiles. The only difficulty is the averaging of the walkoff term $\Delta(u^* u_X - uu_X^*)$, as the walkoff Δ depends on (X, Y) through the temperature (17). To enable the averaging integral to be calculated, we note that the change due to temperature of the refractive indices n_{\parallel} and n_{\perp} is small compared to the initial values [35]. We then expand the walkoff Δ in a Taylor series in τ

$$\begin{aligned} \Delta &= \Delta(\theta_0, T_0) + \left. \frac{\partial \Delta}{\partial T} \right|_{T=T_0} \tau + \dots \\ &= \Delta(\theta_0, T_0) \\ &\quad + \frac{4n_{\parallel 0} n_{\perp 0} (n_{\perp 0} \frac{dn_{\parallel 0}}{dT} - n_{\parallel 0} \frac{dn_{\perp 0}}{dT}) \sin 2\theta_0}{[n_{\parallel 0}^2 + n_{\perp 0}^2 + (n_{\parallel 0}^2 - n_{\perp 0}^2) \cos 2\theta_0]^2} \tau + \dots, \end{aligned} \quad (22)$$

where τ is given by (17) and the 0 subscripts on the refractive indices denote that these are evaluated at $T = T_0$. Despite this approximation, the average of $\Delta(u^* u_X - uu_X^*)$ is too involved to calculate, even if f_e is assumed to be a Gaussian (15). We note that the nondimensional conductivity μ is large, $O(100)$, for typical experiments, as found by using the parameter values found in Ref. [35] and the NLC thermal parameter values found in Ref. [45]. Therefore, the width w of the light beam is much narrower than the width of the temperature response of the medium, in much the same manner in which the NLC reorientational response is nonlocal [6]. Hence, in averaging $\Delta(u^* u_X - uu_X^*)$, the value of τ at the center of the beam can be taken. With these assumptions, averaging (18) gives the averaged Lagrangian \mathcal{L}

$$\begin{aligned} \mathcal{L} &= -2a^2 w^2 S_2 (\sigma' - V\xi') \\ &\quad - 2a^2 w^2 S_2 \gamma \left(\Delta(\theta_0, T_0) + \left. \frac{\partial \Delta}{\partial T} \right|_{\tau=0} \frac{a^2 w^2 C_1}{4\mu} \right) V \\ &\quad - a^2 S_{22} - a^2 w^2 S_2 V^2 - 4\nu S_{42} a_d^2 \\ &\quad + 4a^2 w^2 a_d S_m \left(1 + \left. \frac{d\epsilon_a}{dT} \right|_{\tau=0} \frac{a^2 w^2 C_1}{4(\epsilon_a)_t \mu} \right), \end{aligned} \quad (23)$$

where the various integrals involved are

$$\begin{aligned} S_2 &= \int_0^\infty \zeta f_e^2(\zeta) d\zeta, \quad S_{22} = \int_0^\infty \zeta f_e'^2(\zeta) d\zeta, \\ S_{42} &= \frac{1}{4} \int_0^\infty \zeta \left[\frac{d}{d\zeta} f_d(\zeta) \right]^2 d\zeta, \\ S_m &= \int_0^\infty \zeta f_e^2(\zeta) f_d \left(\frac{w}{w_d} \zeta \right) d\zeta, \end{aligned} \quad (24)$$

and

$$C_1 = \int_0^{\sqrt{2} \frac{R}{w}} \frac{1 - e^{-\eta^2}}{\eta} d\eta. \quad (25)$$

The exact values of these integrals are not needed to calculate the nematicon trajectory. The only assumption needed for

the nematicon solution is the Gaussian approximation (15) to calculate the beam-induced temperature change.

As a nematicon propagates, its amplitude a and width w oscillate and evolve to a steady state. However, it has been found [13,16,20] that this amplitude or width evolution decouples from the trajectory evolution owing to the highly nonlocal response [6]. The main effect of the nematicon amplitude or width oscillations is the shedding of diffractive radiation, enabling the solitary wave to reach a steady state. For a large nonlocality ν the shed radiation has low amplitude and is emitted on a long Z scale [9,13], so that the approach to a steady state is gradual. Physically, a high nonlocality gives rise to a very wide potential well around the evolving nematicon, which essentially traps the radiation. As we are only interested in the nematicon trajectory, we shall assume constant values for the nematicon amplitude a and width w , as well as the amplitude a_d and width w_d of the molecular director distribution. Taking the beam and director amplitudes and widths as constants, variations of the averaged Lagrangian (23) with respect to η and V give the equations for the beam trajectory as

$$V' = 0, \quad (26)$$

$$\xi' = V + \gamma \left[\Delta(\theta_0, T_0) + \frac{\partial \Delta}{\partial T} \Big|_{T=T_0} \frac{a^2 w^2 C_1}{4\mu} \right]. \quad (27)$$

The transverse velocity V is constant, with $V = 0$ since the beam is launched along z , as in the experiments [35]. Integrating the trajectory equation (27) and reverting back to dimensional coordinates using (6), (7), (11), (12), and (14) gives the dimensional trajectory ξ_{dim} of the optical wave packet as

$$\xi_{\text{dim}} = \left[\Delta(\theta_0, T_0) + \frac{\partial \Delta}{\partial T} \Big|_{T=T_0} \frac{\alpha C_1}{2\pi S} P \right] z, \quad (28)$$

where the beam power is

$$P = \Gamma \int_{-\infty}^{\infty} \int_{-\infty}^{\infty} |E|^2 dx dy. \quad (29)$$

To calculate the beam trajectory from (28), using (22) for the temperature derivative of Δ , the temperature dependence of the refractive indices n_{\parallel} and n_{\perp} are needed. The experimental work of the authors of Ref. [35] gives data for these dependencies. It was found that a cubic polynomial fit in temperature T

$$n_{\parallel} = \beta_{\parallel 0} + \beta_{\parallel 1} T + \beta_{\parallel 2} T^2 + \beta_{\parallel 3} T^3, \quad (30)$$

$$n_{\perp} = \beta_{\perp 0} + \beta_{\perp 1} T + \beta_{\perp 2} T^2 + \beta_{\perp 3} T^3 \quad (31)$$

provides an excellent match to these dependencies, as shown in Fig. 2. The coefficients of these interpolating polynomials are given in Table I.

To compare the trajectories given by (28) to experimental results, values of the parameters in this solution are needed. For the thermal absorption coefficient α for the NLC mixture E7 we use the typical value $\alpha = 10 \text{ m}^{-1}$ [45]. In addition, the E7 thermal conductivity is $S = 0.7 \text{ Wm}^{-1} \text{ K}^{-1}$ [45]. The experiments of the authors of Ref. [35] used a beam of waist

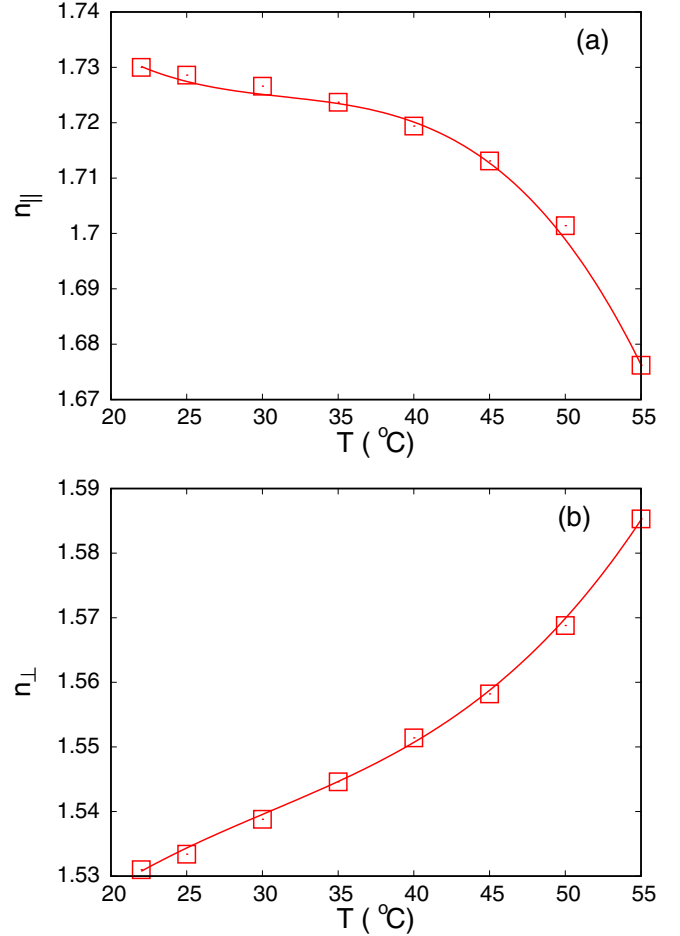


FIG. 2. Comparison between the experimental data for (a) n_{\parallel} and (b) n_{\perp} as a function of temperature in E7 [35] and the interpolating polynomials (30) and (31). Experimental data: squares; interpolating polynomials: solid lines.

$3 \mu\text{m}$. If we take the waist of the beam to be the radius r at which (19) falls to 0.01 of its center value, this gives $w = 1.5 / \ln 10$. Hence, as the half width of the experimental cell was $50 \mu\text{m}$, this gives $R/w = 50 \ln 10 / 1.5 = 76.75$, so that the integral (25) is $C_1 = 4.98$.

The comparisons between the simulated trajectories and the experimental data require the acquisition of the beam path versus propagation distance for various input powers and sample temperatures. Such systematic work can only be conducted in temperature controlled and temperature stabilized NLC samples with the molecular director distribution in the observation plane (x, z) , i.e., the plane parallel to the planar interfaces defining the cell. This last yields beam trajectories

TABLE I. Coefficients of interpolating cubic polynomials (30) and (31) based on the experimental data found in Ref. [35].

$\beta_{\parallel 0}$	$\beta_{\parallel 1}$	$\beta_{\parallel 2}$	$\beta_{\parallel 3}$
1.832	-9.642×10^{-3}	2.973×10^{-4}	-3.152×10^{-6}
$\beta_{\perp 0}$	$\beta_{\perp 1}$	$\beta_{\perp 2}$	$\beta_{\perp 3}$
1.47	4.908×10^{-3}	-1.285×10^{-4}	1.406×10^{-6}

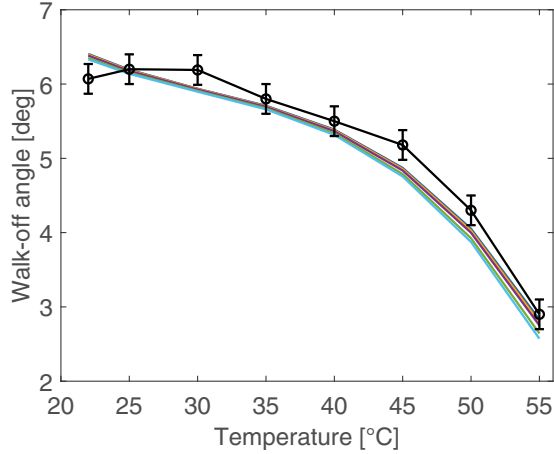


FIG. 3. Comparison between the experimental data (symbols) of Ref. [35] for the beam walkoff angle and the results of the model (28) (color lines), at various temperatures between 22° and 55°. The experimental results were averaged over various input powers at 1.064 μm . The error bars resulted from transverse fluctuations of the beam, as well as the limited accuracy of the setup. Color lines are (28) for beam powers 2, 4, 5, 7.5, 15, and 20 mW (from top to bottom), respectively.

and walkoff in (x, z) , in such a way that out-of-plane light scattering can provide a means for acquiring photographs with a microscope and a camera mounted with axes along the y direction. This analysis was conducted by Laudyn and coworkers, as detailed in Ref. [35]. It should be noted that there were errors in the reporting of the experimental results in Ref. [35], which were corrected in the erratum [46]. In checking the validity of the simulation results against laboratory data, a few issues have to be underlined beyond the approximations introduced in the model and discussed above. Experiments are subject to nonlinear changes in walk-off versus input power, as well as scattering losses. These two effects can cause a significant distortion of the trajectories from rectilinear paths, as the beam power decays versus propagation. The model detailed in the present paper accounts for the nonhomogeneous temperature changes due to absorption and heating along or across the beam, but neglects the reorientation driven changes to the walkoff. Figure 3 shows the calculated walkoff angle versus sample temperature for various input powers as compared with an average of the experimental results [35]. The experimental data are derived from the initial paths of the nematicons to reduce the influence of beam attenuation and the resulting change in walkoff angle. The latter values are obtained from photographs of beam evolution at a wavelength of 1.064 μm in 100- μm -thick E7 samples with the molecular director set by anchoring at 60° in (x, z) with respect to the input wave-vector \mathbf{k} parallel to z [35] (see Fig. 1). The transverse fluctuations of the nematicons [31,47], as well the limitations of the setup and temperature controller and stabilizer, are accounted for by error bars. The walkoff angles were averaged over several input powers between 2 and 20 mW. The agreement between the analytical model and the experiments is remarkably good, in spite of the aforementioned shortcomings.

TABLE II. Initial walkoff angle δ in degrees as given by (a) experimental results found in Ref. [35], (b) theoretical angle (28), ξ'_{dim} , at $z = 0$.

Beam power mW	40 °C	45 °C	50 °C	55 °C
(a)				
7.5	5.53	5.19	4.33	2.95
15	5.81	5.19	3.93	2.59
20	5.33	5.08	3.82	2.46
(b)				
7.5	5.37	4.84	4.00	2.75
15	5.34	4.79	3.92	2.64
20	5.32	4.76	3.87	2.57

It can be seen from Fig. 3 that the walkoff angle only shows significant dependence on beam power at high powers and at the upper end of the temperature range. This is because the physical properties of E7 are dependent on temperature due to its weak optical absorption [45]. Table II shows comparisons between the initial walkoff angle ($z = 0$) as obtained from the experimental results of [35] in (a) and the angle as calculated from (28) for a moderate power 7.5 mW and the two high powers 15 and 20 mW in (b). The experimental results found in Ref. [35] and the theoretical walkoff results of Fig. 3 show that there is significant walkoff deviation with power above 45 °C and for the beam powers 15 and 20 mW. It can be seen that the theoretical results are in good agreement with experimental results at 50° and 55 °C for the higher powers. The agreement at the lower temperatures and the moderate power 7.5 mW is reasonable, given the approximations mentioned above. The experimental results of Table II(a) at the lower power 7.5 mW and the lower temperatures show significant nonmonotonic variation, which is presumably due to the experimental limitations mentioned above. Hence close agreement cannot be expected for these temperatures and powers.

III. CONCLUSION

This study emphasizes and confirms the power of modulation theory and averaged Lagrangian analyses for modeling light beam evolution in nematic liquid crystals [7,9,11–24]. This study has only touched on the effects of the temperature dependence of the NLC physical properties on nematicon propagation and leaves a large number of questions open, including the role of such nonlinear synergy or competition on multihumped, two-dimensional nematicon profiles, power-dependent walkoff, nonlocal effects, and so on. Several such investigations are underway.

ACKNOWLEDGMENTS

We acknowledge the sample preparation and the experimental measurements carried out at the Faculty of Physics of the Warsaw University of Technology by U. Laudyn, M. Kwasny, and M. Karpierz and reported in Ref. [35]. A.P.'s work was supported by grant National Program of Military Research No. a2016.005.

- [1] I. Khoo, *Liquid Crystals: Physical Properties and Nonlinear Optical Phenomena* (John Wiley and Sons, New York, 2007).
- [2] M. Peccianti and G. Assanto, Nematic Liquid Crystals: a suitable medium for self-confinement of coherent and incoherent light, *Phys. Rev. E* **65**, 035603(R) (2002).
- [3] G. Assanto and M. Peccianti, Spatial solitons in nematic liquid crystals, *IEEE J. Quantum Electron.* **39**, 13 (2003).
- [4] G. Assanto and M. Karpierz, Nematicons: self-localized beams in nematic liquid crystals, *Liq. Cryst.* **36**, 1161 (2009).
- [5] G. Assanto, Nematicons: reorientational solitons from optics to photonics, *Liq. Cryst. Rev.* **6**, 170 (2018).
- [6] M. Peccianti and G. Assanto, Nematicons, *Phys. Rep.* **516**, 147 (2012).
- [7] G. Assanto, *Nematicons, Spatial Optical Solitons in Nematic Liquid Crystals* (John Wiley and Sons, New York, 2012).
- [8] C. Conti, M. Peccianti, and G. Assanto, Route to Nonlocality and Observation of Accessible Solitons, *Phys. Rev. Lett.* **91**, 073901 (2003).
- [9] A. A. Minzoni, N. F. Smyth, and A. L. Worthy, Modulation solutions for nematicon propagation in non-local liquid crystals, *J. Opt. Soc. Amer. B* **24**, 1549 (2007).
- [10] A. Alberucci and G. Assanto, Propagation of optical spatial solitons in finite size media: Interplay between non local-ity and boundary conditions, *J. Opt. Soc. Am. B* **24**, 2314 (2007).
- [11] G. Assanto, A. A. Minzoni, and N. F. Smyth, Light self-localization in nematic liquid crystals: modeling solitons in nonlocal reorientational media, *J. Nonlin. Opt. Phys. Mater.* **18**, 657 (2009).
- [12] G. Assanto, A. A. Minzoni, M. Peccianti, and N. F. Smyth, Optical solitary waves escaping a wide trapping potential in nematic liquid crystals: Modulation theory, *Phys. Rev. A* **79**, 033837 (2009).
- [13] B. D. Skuse and N. F. Smyth, Interaction of two color solitary waves in a liquid crystal in the nonlocal regime, *Phys. Rev. A* **79**, 063806 (2009).
- [14] A. Alberucci, G. Assanto, D. Buccoliero, A. S. Desyatnikov, T. R. Marchant, and N. F. Smyth, Modulation analysis of boundary induced motion of nematicons, *Phys. Rev. A* **79**, 043816 (2009).
- [15] G. Assanto, B. D. Skuse, and N. F. Smyth, Solitary wave propagation and steering through light-induced refractive potentials, *Phys. Rev. A* **81**, 063811 (2010).
- [16] G. Assanto, A. A. Minzoni, N. F. Smyth, and A. L. Worthy, Refraction of nonlinear beams by localised refractive index changes in nematic liquid crystals, *Phys. Rev. A* **82**, 053843 (2010).
- [17] G. Assanto, C. García-Reimbert, A. A. Minzoni, N. F. Smyth, and A. L. Worthy, Lagrange solution for three wavelength solitary wave clusters in nematic liquid crystals, *Physica D* **240**, 1213 (2011).
- [18] A. A. Minzoni, L. W. Sciberras, N. F. Smyth, and A. L. Worthy, Propagation of optical spatial solitary waves in bias-free nematic liquid crystal cells, *Phys. Rev. A* **84**, 043823 (2011).
- [19] G. Assanto, N. F. Smyth, and W. Xia, Modulation analysis of nonlinear beam refraction at an interface in liquid crystals, *Phys. Rev. A* **84**, 033818 (2011).
- [20] A. Alberucci, G. Assanto, A. A. Minzoni, and N. F. Smyth, Scattering of reorientational optical solitary waves at dielectric perturbations, *Phys. Rev. A* **85**, 013804 (2012).
- [21] A. A. Minzoni, L. W. Sciberras, N. F. Smyth, and A. L. Worthy, Nonlinear optical beams in bounded nematic liquid crystal cells, *ANZIAM J.* **53**, 373 (2012).
- [22] A. A. Minzoni, L. W. Sciberras, N. F. Smyth, and A. L. Worthy, Elliptical optical solitary waves in a finite nematic liquid crystal cell, *Physica D* **301–302**, 59 (2015).
- [23] N. F. Smyth and B. Tope, Beam on beam control: Beyond the particle approximation, *J. Nonlin. Opt. Phys. Mater.* **25**, 1650046 (2016).
- [24] G. Assanto and N. F. Smyth, Self confined light waves in nematic liquid crystals, *Physica D* (to be published).
- [25] J. M. L. MacNeil, N. F. Smyth, and G. Assanto, Exact and approximate solutions for optical solitary waves in nematic liquid crystals, *Physica D* **284**, 1 (2014).
- [26] C. Conti, M. Peccianti, and G. Assanto, Complex dynamics and configurational entropy of spatial optical solitons in nonlocal media, *Opt. Lett.* **31**, 2030 (2006).
- [27] A. Alberucci and G. Assanto, Dissipative self-confined optical beams in doped nematic liquid crystals, *J. Nonlin. Opt. Phys. Mater.* **16**, 295 (2007).
- [28] I. B. Burgess, M. Peccianti, G. Assanto, and R. Morandotti, Accessible Light Bullets via Synergetic Nonlinearities, *Phys. Rev. Lett.* **102**, 203903 (2009).
- [29] M. Peccianti, I. B. Burgess, G. Assanto, and R. Morandotti, Space-time bullet trains via modulation instability and nonlocal solitons, *Opt. Express* **18**, 5934 (2010).
- [30] P. S. Jung, W. Krolikowski, U. A. Laudyn, M. Trippenbach, and M. A. Karpierz, Supermode spatial optical solitons in liquid crystals with competing nonlinearities, *Phys. Rev. A* **95**, 023820 (2017).
- [31] S. Bolis, S.-P. Gorza, S. J. Elston, K. Neyts, P. Kockaert, and J. Beeckman, Spatial fluctuations of optical solitons due to long-range correlated dielectric perturbations in liquid crystals, *Phys. Rev. A* **96**, 031803(R) (2017).
- [32] A. Alberucci, C. P. Jisha, S. Bolis, J. Beeckman, and S. Nolte, Interplay between multiple scattering and optical nonlinearity in liquid crystals, *Opt. Lett.* **43**, 3461 (2018).
- [33] U. A. Laudyn, M. Kwasny, A. Piccardi, M. Karpierz, R. Dabrowski, O. Chojnowska, A. Alberucci, and G. Assanto, Nonlinear competition in nematicon propagation, *Opt. Lett.* **40**, 5235 (2015).
- [34] A. Alberucci, U. A. Laudyn, A. Piccardi, M. Kwasny, B. Klus, M. A. Karpierz, and G. Assanto, Nonlinear continuous-wave optical propagation in nematic liquid crystals: interplay between reorientational and thermal effects, *Phys. Rev. E* **96**, 012703 (2017).
- [35] U. A. Laudyn, A. Piccardi, M. Kwasny, M. A. Karpierz, and G. Assanto, Thermo-optic soliton routing in nematic liquid crystals, *Opt. Lett.* **43**, 2296 (2018).
- [36] G. B. Whitham, *Linear and Nonlinear Waves* (J. Wiley and Sons, New York, 1974).
- [37] Y. Izdebskaya, W. Krolikowski, N. F. Smyth, and G. Assanto, Vortex stabilization by means of spatial solitons in nonlocal media, *J. Opt.* **18**, 054006 (2016).
- [38] A. Piccardi, A. Alberucci, and G. Assanto, Soliton self deflection via power-dependent walk-off, *Appl. Phys. Lett.* **96**, 061105 (2010).

- [39] A. Piccardi, A. Alberucci, and G. Assanto, Self-turning Self-Confined Light Beams in Guest-Host Media, *Phys. Rev. Lett.* **104**, 213904 (2010).
- [40] U. A. Laudyn, M. Kwaśny, F. A. Sala, M. A. Karpierz, N. F. Smyth, and G. Assanto, Curved optical solitons subject to transverse acceleration in reorientational soft matter, *Sci. Rep.* **7**, 12385 (2017).
- [41] F. A. Sala, N. F. Smyth, U. A. Laudyn, M. A. Karpierz, A. A. Minzoni, and G. Assanto, Bending reorientational solitons with modulated alignment, *J. Opt. Soc. Am. B* **34**, 2459 (2017).
- [42] U. A. Laudyn, M. Kwaśny, M. A. Karpierz, N. F. Smyth, and G. Assanto, Accelerated optical solitons in reorientational media with transverse invariance and longitudinally modulated birefringence, *Phys. Rev. A* **98**, 023810 (2018).
- [43] D. J. Kaup and A. C. Newell, Solitons as particles, oscillators, and in slowly changing media: a singular perturbation theory, *Proc. Roy. Soc. Lond. A* **361**, 413 (1978).
- [44] B. Malomed, Variational methods in nonlinear fiber optics and related fields, *Prog. Opt.* **43**, 71 (2002).
- [45] I. C. Khoo, Principal nonresonant optical nonlinearities of nematic and isotropic liquid crystals, in *Nonlinear Optics and Optical Physics*, edited by F. Simoni, I.-C. Khoo, and J.-F. Lam, Series in Nonlinear Optics Vol. 2 (World Scientific, Singapore, 1994), pp. 176–210.
- [46] U. A. Laudyn, A. Piccardi, M. Kwasny, M. A. Karpierz, and G. Assanto, Thermo-optic soliton routing in nematic liquid crystals: erratum, *Opt. Lett.* **44**, 2268 (2019).
- [47] U. A. Laudyn, M. Kwasny, M. Karpierz, and G. Assanto, Electro-optic quenching of nematicon fluctuations, *Opt. Lett.* **44**, 167 (2019).